NASA Technical Memorandum 83088
AIAA-83-0537

Flight Evaluation of Modifications to a Digital Electronic Engine Control System in an F-15 Airplane

Frank W. Burcham, Jr. and Lawrence P. Myers
Hugh L. Dryden Flight Research Facility
Edwards, California

and

John R. Zeller
Lewis Research Center
Cleveland, Ohio

Prepared for the
Twenty-First Aerospace Sciences Conference
sponsored by the American Institute of
Aeronautics and Astronautics
Reno, Nevada, January 10-13, 1983

NASA

As a result of the Phase 2 evaluation, and on-going development of the DEEC system, a series of engine and control system modifications were developed for Phase 3 flight evaluation. The nozzle instability had not been predicted from previous engine tests and could not be duplicated with engine simulations. Therefore, a series of tests were conducted at NASA Lewis Research Center to generate data to improve the engine simulations and to evaluate potential logic changes to eliminate the instability.

This paper presents the analysis and simulation results for the nozzle instability, the control system and engine hardware and software modifications, and results of the Phase 3 flights.

Airplane

The F-15 airplane is a high-performance, twin-engine fighter, capable of speeds to Mach 2.5. The engine inlets are of the two-dimensional external compression type with three ramps, and feature variable capture area. The F-15 is powered by two F100-PW-100 engines. The DEEC test engine was installed in the left side of the F-15. An unmodified F100 engine was installed in the right side.

Engine Description

The F100-PW-100 engine (Fig. 1) is a low-bypass-ratio (0.8), twin-spool, afterburning turbofan. The three-stage fan is driven by a two-stage, low-pressure turbine. The engine is equipped with a proximate splitter - a fan-core flow divider that extends to the fan discharge. The 10-stage, high-pressure compressor is driven by a two-stage high-pressure turbine. The engine incorporates compressor inlet variable vanes (CIVV) and rear compressor variable vanes (RCVV) to achieve high performance over a wide range of power settings; a compressor bleed is used only for starting. Continuously variable thrust augmentation is provided by a mixed-flow-augmentor, which is exhausted through a variable-area convergent-divergent nozzle. The augmentor incorporates five spray ring segments which are ignited sequentially. Segments 1, 2, and 4 are located in the core stream, and segments 3 and 5 are located in the fan duct stream. The augmentor was equipped with dual-augmentor ignitors, whereas the standard F100 engine has only one. It also had a ducted core flameholder, which ducts a small amount of hot core-flow to the flameholders located in the fan duct stream. The standard F100 engine flameholder does not duct any core air to the fan duct stream. In the latter part of Phase 3, the ducted core flame holder was replaced with a standard F100 flame holder. The engine was also equipped with an engine hub mounted static pressure probe (PS2), used to provide a control signal. The PS2 probe is not present on the standard F100 engine.

The F100 engine used for the DEEC flight evaluation was S/N 680063. It had been rebuilt from an earlier F100(2) engine to a zero-time F100 (3) configuration with the DEEC system before the DEEC flights. The engine had accumulated 9.8 hr of sea level testing and 45.4 hr at an altitude facility before the first DEEC flights.

The F100 engine used for the DEEC nozzle instability testing at the NASA Lewis Research Center was S/N XD-11, a research engine with some components that are modified from the standard F100 configuration.

Control System Description

DEEC. The DEEC is a full-authority, engine-mounted, fuel-cooled digital electronic control system that performs the functions of the standard F100 engine hydromechanical unified fuel control and the supervisory digital engine electronic control. The DEEC consists of a single-channel digital controller with selective input-output redundancy, and an integral simple hydromechanical backup control (BUC). The DEEC system is functionally illustrated in Fig. 2. It receives inputs from the airframe through throttle position (PLA) and Mach number (M), and from the engine through rotor speed sensors (N1, N2), temperature sensors (TT2, FTIT), and pressure sensors (PS2, PB, PT6M). The engine mounted alternator provides electrical power to the DEEC in addition to the N2 signal. The DEEC receives feedbacks from the controlled variables through position feedback transducers indicating variable vane (CIVV, RCVV) positions, metering valve positions for gas-generator fuel flow (WFGG), augmentor core and duct fuel flow, segment sequence valve position, and exhaust nozzle position (AJ). Dual sensors and position transducers are used as shown to achieve redundacy in key parameters.

The input information is processed by the DEEC computer to schedule the variable vanes (CIVV, RCVV), to position the compressor start bleeds, to control gas-generator and augmentor fuel flows, to position the augmentor segment-sequence valve, and to control exhaust nozzle area. Dual coils are used in the torque motors that drive the servo valves for all of the actuators.

DEEC logic. The DEEC logic provides openloop scheduling of CIVV, RCVV, start bleed position, and augmentor controls. The DEEC incorporates closed-loop control logic to eliminate the need for periodic trimming and to improve performance. The two basic closed loop control modes are shown in Fig. 3. The top part of the figure shows the N1 logic in which gas-generator fuel flow (WFGG) is controlled to maintain the scheduled fan speed (N1) and hence, airflow. Proportional-plus-integral control is used to match the measured N1 to the requested N1. Limits of N2, FTIT, and PB are maintained. The N1 loop is used for all throttle settings.

Shown in the lower part of Fig. 3 is the engine pressure ratio (EPR) loop. The requested EPR is compared with the measured EPR, based on PT2 and PT6M. The PT2 signal is derived from the PS2 measurement. A PT2-PS2 relationship has been determined from previous wind-tunnel and flight tests.[4] Using proportional-plus-integral control, DEEC modulates the nozzle to achieve the requested EPR. The EPR control loop is only active for intermediate power operation and augmentation. At lower power settings, a scheduled nozzle area is used.

With the closed-loop N1 and EPR logic, the DEEC control is capable of automatically compensating for engine degradation. EPR is directly related to thrust, so the DEEC can maintain an engine at a desired thrust level. As the engine degrades, the FTIT required to achieve the scheduled EPR will increase until it reaches its limit. The DEEC will then operate the engine on the FTIT limit.

Augmentor logic. Augmentor fuel distribution is handled by a segment-sequencing valve and the core and duct fuel metering valves (Fig. 2). Each of the five segments has a hydromechanical "quickfill" feature, which supplies a high fuel-flow rate to rapidly fill the fuel manifold and spray ring. A mechanical quickfill sensor determines when each segment is full by the rise in fuel pressure, turns off the quickfill fuel flow to that segment, and transfers that segment to the metered fuel flow scheduled by the DEEC computer. The segment-sequencing valve handles the sequencing of quick-fill and metered flow, and the separate core and duct fuel-flow metering valves control the flow to the segments.

The DEEC incorporates a maximum segment-1 limiting feature in the upper left-hand corner of the flight envelope. This limits the augmentor sequencing to the maximum segment-1 fuel flow, even though a higher power setting has been requested. In addition, an override switch was installed in the cockpit for this flight evaluation; making it possible to override the maximum segment-1 limit and achieve full augmentation.

Backup control (BUC). The backup control in the DEEC system is a simple hydromechanical engine control housed in the same unit as the DEEC gas generator fuel-metering valves. BUC operation is limited to nonaugmented power and is operable over the entire engine operating envelope. If DEEC control capability is lost, a spring-loaded transfer valve is positioned such that the BUC components will control WFGG, RCVV, and start bleeds. The CIVVs go full cambered, the nozzle closes, and augmentation is cancelled. BUC inputs are PS2, TT2, PLA, and RCVV position. In BUC operation, at intermediate power, the engine will generally produce lower thrust than in the DEEC mode. Airstarts may be made in BUC mode; moving the throttle from cutoff to idle initiates a timed fuel flow ramp, which is biased by PS2. When the start timer elapses, the compressor start bleeds close, the RCVVS are scheduled, and BUC idle fuel flow is scheduled. The BUC start timer duration was 40 sec for Phase 1 and 2, and was lengthened to 70 sec for Phase 3. Additional information on the DEEC and BUC is given in Ref. 3.

Data Acquisition And Reduction

Pressures, temperatures, rotor speeds, fuel flows, and positions were measured on the DEEC test engine. In addition, a 50-word serial digital data stream from the DEEC computer was recorded. Angle of attack and sideslip, noseboom total and static pressure, and other aircraft parameters were measured. Data were recorded on a pulse code modulation (PCM) system. High-frequency response parameters, such as PB, PAB, PT2, and the augmentor segment fuel pressures, were recorded at 200 samples/sec; the other engine and aircraft parameters were recorded at 20 samples/sec. The DEEC digital data stream was updated at 8 samples/sec. The various parameters were filtered before digitization by the PCM system to prevent aliasing error. The data were recorded on a tape recorder on the F-15 and also were telemetered to the ground for recording and for real-time analysis and display.

Tests And Procedures

Flight Evaluation

The DEEC flight evaluation has consisted of 25 flights, including seven during Phase 3, for a total flight time of 29.8 hr. Included are over 800 augmentor transients, 150 airstarts, over 200 nonaugmented transients, backup control system evaluations, maneuvering flights, accelerations, and climbs. A maximum Mach number of 2.36 was reached and a minimum airspeed of 99 kts at an altitude of 25 000 ft was achieved. Climbs were made to 60 000 ft to evaluate the upper limits of augmentor operation. For other test points in which stabilized speed and altitude were required, the pilot used the right engine to control speed while the left DEEC test engine was evaluated. In maneuvering flight, large angles of attack and sideslip (up to about 25° and 15°, respectively) were flown, and throttle transients were performed. Reference 2 describes the test procedures in more detail.

For augmented throttle transients, a series consisted of an intermediate-to-maximum-to-intermediate throttle sequence, followed by idle-to-maximum-to-idle snaps. No attempt was made to allow the augmentor manifolds to drain completely between transients. When stalls or blowouts occurred at a given test point, the transient was repeated until the same result was achieved in two out of three trials. Augmentor transients were performed in the upper left-hand corner with maximum segment-1 limiting. Using the override switch, transients to full augmentation were also performed.

For airstarts, the pilot set up at the desired test condition, advanced the throttle to intermediate power to provide repeatable initial conditions, and then shutdown the engine. As the engine spooled down to the desired N2 speed, the pilot moved the throttle to idle to initiate airstart. Speed and altitude were maintained using the right engine until the test engine reached idle rpm, or until an unsuccessful airstart was evident. Unsuccessful airstarts were indicated either by increasing FTIT with decreasing N2 (hot start), or a very slow or zero rate of increase in N2 (hung start). All airstarts were performed with the normal F-15 bleed and accessory loads.

Altitude Facility Tests

A series of altitude test runs were performed at the Lewis Research Center to investigate the possible cause of the nozzle instability which occurred during the second phase of DEEC flight testing at Dryden. The testing was performed in the upper left-hand corner (low speed/high altitude) of the flight envelope with the augmentor in operation since this is where the instability was encountered. The engine used was the F100 XD-11 test engine controlled by the DEEC breadboard control. Software changes could be entered via tape or a keyboard. The DEEC breadboard was used to execute a matrix of different EPR loop control parameter settings. The parameters to be varied were 1) integrator gain, 2) proportional gain, and 3) insertion of a pure deadband in the EPR

control loop. Step inputs to the EPR loop were used predominantly to evaluate the nozzle control's transient performance for the various parameter settings. Once a set of control parameters was found which produced an oscillatory system response, frequency response tests were run. Sinewave inputs of selected amplitude and frequency were produced by the DEEC breadboard and interjected into the system. This data was intended to provide transfer function data for control system analysis. This would enable refinements to the EPR loop model and selection of improved control settings. Data was also obtained using large power lever angle inputs in and out of augmentor operation.

Results And Discussion

The discussion following first summarizes the Phase 2 augmentor transient performance limits. Then the nozzle instability flight data, altitude tests, simulation results and logic changes are discussed. Then, the Phase 3 results are compared to Phase 2, including nozzle stability, quickfill stalls, rumble blowouts, and backup control system airstart improvements.

Augmentor Transient Performance

Phase 2 results summary. Augmentor transient performance limits determined during DEEC Phase 2 flights are shown in Fig. 4. Augmentor transients caused stalls and blowouts as indicated in Fig. 4(a), for intermediate-to-maximum power snap throttle transients, and in Fig. 4(b), for idle-to-maximum power snap transients. Analysis showed that a nozzle instability, augmentor rumble, and quickfill spikes, contributed to many of these augmentor anomolies.[3] The Phase 3 flights evaluated changes to the control and augmentor hardware to reduce or eliminate these anomolies.

Nozzle instability. An example of the nozzle instability encountered in Phase 2 at an altitude of 50 000 ft and an airspeed of 200 knots is shown in Fig. 5. Following an intermediate-to-maximum power throttle transient, the nozzle oscillated in a limit cycle with an amplitude of approximately 0.2 ft^2 at a frequency of approximately 1.5 Hz. Some nozzle over-and-undershoots also occurred during the augmentor sequencing. Also shown is the augmentor high frequency response static pressure, PAB. The instability resulted in an augmentor blowout, caused by the low PAB level that occurred when the nozzle was too far open.

An example of a stall that occurred as a result of nozzle instability following an idle-to-maximum throttle transient at 175 knots, 45 000 ft is shown in Fig. 6. The nozzle oscillation built up over a period of 4 cycles and the high pressure level back pressured the fan, causing the stall.

In other instances, the oscillation began, damped out, and began again, indicating a marginal stability in the nozzle control loop. The oscillation only occurred for augmented power, not at intermediate power. As shown in Fig. 3, the nozzle is controlled to maintain the desired engine pressure ratio, EPR. During the DEEC design and initial evaluation, the stability of the EPR control loop was evaluated and found to be adequate, based on simulation results. During flight clearance testing at Arnold Engineering and Development Center (AEDC), the EPR loop stability of the DEEC flight test engine (S/N P680063) was evaluated at low airspeed -- high altitude conditions, but only at intermediate power. The nominal EPR loop gain was doubled and no instability was noted.

In order to more exhaustively investigate the causes of the EPR control loop nozzle instability, the altitude test program mentioned earlier was performed at the NASA Lewis Research Center. The F100 XD-11 engine used for this test did not exhibit any nozzle stability problems when operating with its normal control gain settings. Thus the DEEC breadboard was used to provide variable gain and other control modifications. During the program it was found that an increase in integral control gain could cause the nozzle to become oscillatory at a M = 0.6, 45 000 ft altitude condition, Fig. 7. Fig. 7(a) is a plot representative of the type of results obtained with the integral gain 2.5 times nominal. This figure shows that there are lightly damped 1.4 Hz oscillations (ringings) of ± 0.1 ft^2 amplitude when a small step change in EPR command is initiated and removed. Fig. 7(b) shows this result more dramatically for an integral gain increase to 3.5 times nominal. In both of these cases, the oscillations damped within a few seconds. These results were obtained with the deadband element in the EPR control loop set to zero. A small deadband element was included in the DEEC software used for the Phase 2 flight tests. This resultant instability, produced by the increased integral gain, does not demonstrate the sustained oscillations of the flight test results of Figs. 5 and 6. This just indicates there are probably mechanical differences between XD-11 and the flight test engine in areas such as friction, rigging tolerances and wear. The important fact is that the frequencies of oscillation are very close indicating comparable linear dynamic properties. This fact makes further analysis of the data meaningful. Frequency response data useful for a linear model analysis was obtained during the altitude tests by inserting different frequency sinewave EPR commands.

With the results of the NASA Lewis tests, it was practical to improve the engine simulation. The engine manufacturer conducted a linear system analysis of the EPR control loop and found that the loop had very marginal stability at high altitude-low airspeed conditions. It was proposed to cut the EPR loop gain in half and to incorporate a larger deadband in the loop to increase its stability.

To further investigate the nozzle instability, NASA Dryden developed a nonlinear digital simulation of the EPR control loop, incorporating the transfer functions developed from the NASA Lewis test data and the engine manufacturer's linear analysis. A block diagram of the simulation is shown in Fig. 8. It models the part of the EPR control loop of Fig. 3 that is enclosed in the dashed lines. The EPR request is input, passed through a deadband, then to integral and proportional gains to generate the EPR request. This is converted to a nozzle area request, which is input into a nozzle dynamics block. This block includes nozzle rate limiting and hysteresis. The nozzle output is used to generate the appropriate EPR output for the particular flight condition, the AJ/EPR transfer function having been determined from the NASA Lewis test results. The resulting EPR is fed back through the DEEC pressure sensors,

the DEEC computer digital filter, and DEEC computation cycle time to generate the DEEC EPR feedback. Another feedback loop must also be considered. As the nozzle area and EPR changes, the fan speed, N1 responds. As noted in Fig. 3, N1 is an input to the EPR request logic. The AJ/N1 transfer function was derived from Lewis test data. The N1 to EPR constant is the slope of the N1 to EPR table used by the DEEC logic in computing the EPR request.

The simulation was mechanized in the time domain using Z transform techniques. The digital computer program used an integration interval of 0.005 sec, and modeled the DEEC computational cycle time of 0.02 sec. A step input in EPR request was used to evaluate the EPR loop stability.

Results of the Dryden nonlinear EPR loop simulation are shown in Fig. 9 for a M = 0.6, 45,000 ft condition, with the deadband, proportional, and integral gains from the DEEC Phase 2 software. As may be seen in Fig. 9(a), the simulation results show a limit cycle with very similar frequency and magnitude to the nozzle oscillation observed in flight which are also shown in Fig. 9(b). The fact that this simulation, which incorporated the NASA Lewis test results, duplicated the flight results, whereas the engine manufacturer's full dynamic simulation did not, points up the importance of having very high quality engine modeling data.

The engine manufacturer's proposed gain and deadband changes were evaluated on the Dryden simulation and verified that the EPR loop would be stable. These changes were incorporated in the Phase 3 DEEC software logic.

The Phase 3 DEEC flight evaluation has shown no evidence of nozzle instability. The lower EPR loop gain also reduced the nozzle overshoots that occurred during augmentor sequencing, and that reduced the number of blowouts that occurred during augmentor transients.

Rumble blowouts. The rumble induced blowouts that occurred during the DEEC Phase 2 flight evaluation were caused by temporary overrich fuel-air ratios that occurred just as the segment 4 fuel flow reached its full value. An example is shown in Ref. 3. The flight clearance tests at Arnold Engineering and Development Center had not indicated rumble during similar transients. This may have been due to variations in inlet total pressure that occurred in the test facility that did not occur in flight.

The DEEC Phase 3 software was modified to lower the segment 4 fuel-air ratio slightly. No rumble-induced blowouts have been observed during the Phase 3 flight evaluation.

Quickfill spike induced stalls. As shown in Ref. 3, augmentor quickfill fuel spikes occasionally generated augmentor pressure pulses that caused stalls during augmentor throttle transients. The quickfill system is hydromechanical, and DEEC software logic can do nothing to eliminate the quickfill spikes. However, the quickfill system pressure sensor flown in Phase 2 was underdamped, and resulted in high frequency oscillations in segment fuel pressures. This underdamped behavior also made the quickfill spikes more severe. For Phase 3, a quickfill sensor with improved damping characteristics was installed. With this quickfill sensor installed, the high frequency oscillations have been greatly reduced, and the incidence of quickfill stalls has been reduced.

Augmentor flameholder evaluation. During Phase 1 and 2 flight testing, the ducted core flameholder was installed in the augmentor. During the latter part of Phase 3, the standard F100 production flameholder was installed, and augmentor transients were performed. Transient performance was similar, except for intermediate to maximum power transients at an airspeed of 150 knots at an altitude of 45 000 ft, where the production flameholder was successful in 4 of 4 attempts, whereas the ducted core flameholder was only successful in 1 of 3 attempts. Based on the available data, it is concluded that ducted core flameholder is not better, and may be slightly inferior to the production flameholder.

Summary of Phase 3 augmentor changes. The overall augmentor transient performance with the Phase 3 software to eliminate the rumble and nozzle instability, the damped quickfill sensor, and the production flameholder is shown in Fig. 10. The success boundary is shown, along with the success boundary from Phase 2. A significant improvement is shown. For intermediate-to-maximum power transients; Figure 10(a), the improvement is as much as 8000 ft in altitude, while for idle-to-maximum power throttle transients, Fig. 10(b), the altitude improvement is as much as 4000 ft. In addition, no stagnations have occurred in Phase 3, whereas 2 stagnations occurred in Phase 2.

Backup control system airstarts. During the Phase 3 flight evaluation, a series of BUC airstarts have been conducted to evaluate the change from the 40 sec BUC start timer of Phase 2 to the 70 sec start timer of Phase 3. In Phase 3, successful BUC airstarts were accomplished at airspeeds of 200 knots; with some 40 percent spooldown airstarts successful at 175 kts, as shown in Fig. 11. The Phase 2 success line from Ref. 3 is also shown, at approximately 275 knots. The Phase 3 BUC airstart capability at 200 knots is significant considering that the optimum glide speed for the F-15 and F-16 is approximately 200 knots.

Concluding Remarks

A series of modifications to a digital electronic engine control system on an F100 engine have been evaluated in the 3rd phase of a flight evaluation in an F-15 airplane.

It was found that DEEC software logic changes and augmentor hardware changes resulted in significant improvement in augmentor transient capability. For intermediate to maximum power throttle transients, an increase in altitude capability of up to 8000 ft was found. For idle to maximum throttle transients, an increase of up to 4000 ft was found.

A nozzle instability noted in earlier flights was investigated on a test engine at the NASA Lewis Research Center, and a DEEC software logic change was developed and evaluated. A nonlinear digital simulation was developed that nearly duplicated the instability observed in flight. With the software change in Phase 3, no nozzle instability was observed.

The backup control system airstart modification was also evaluated in Phase 3, and gave an improvement in airstart capability by reducing the minimum airspeed for successful airstarts by 50 to 75 knots.

References

1. Barrett, W. J.; Rembold, J. P.; Burcham, F. W., Jr.; and Myers, L.: "Flight Test of a Full Authority Digital Electronic Engine Control System in an F-15 Airplane", AIAA Paper 81-1501, July 1981.

2. Burcham, F. W., Jr.; Myers, L. P.; Nugent, J.; Lasagna, P.; and Webb, L. D.: "Recent Propulsion System Flight Tests at NASA Dryden Flight Research Center", AIAA Paper 81-2438, Nov. 1981.

3. Myers, L.; Mackall, K.; and Burcham, F. W., Jr.: "Flight Test Results of a Digital Electronic Engine Control System in an F-15 Airplane", AIAA Paper 82-1080, June 1982.

4. Foote, C. H.; and Jaekel, R. J.: "Flight Evaluation of an Engine Static Pressue Nose-probe in F-15 Airplane", NASA CR-163109, 1981.

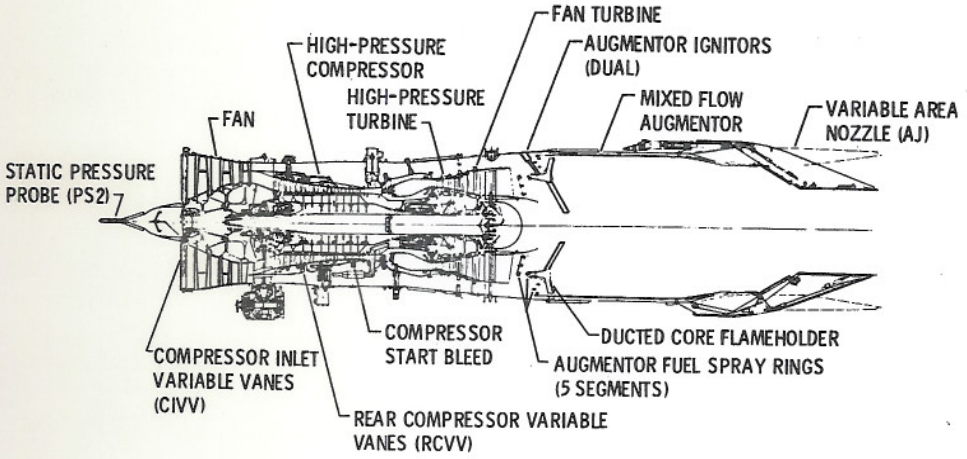

Figure 1. - DEEC test engine.

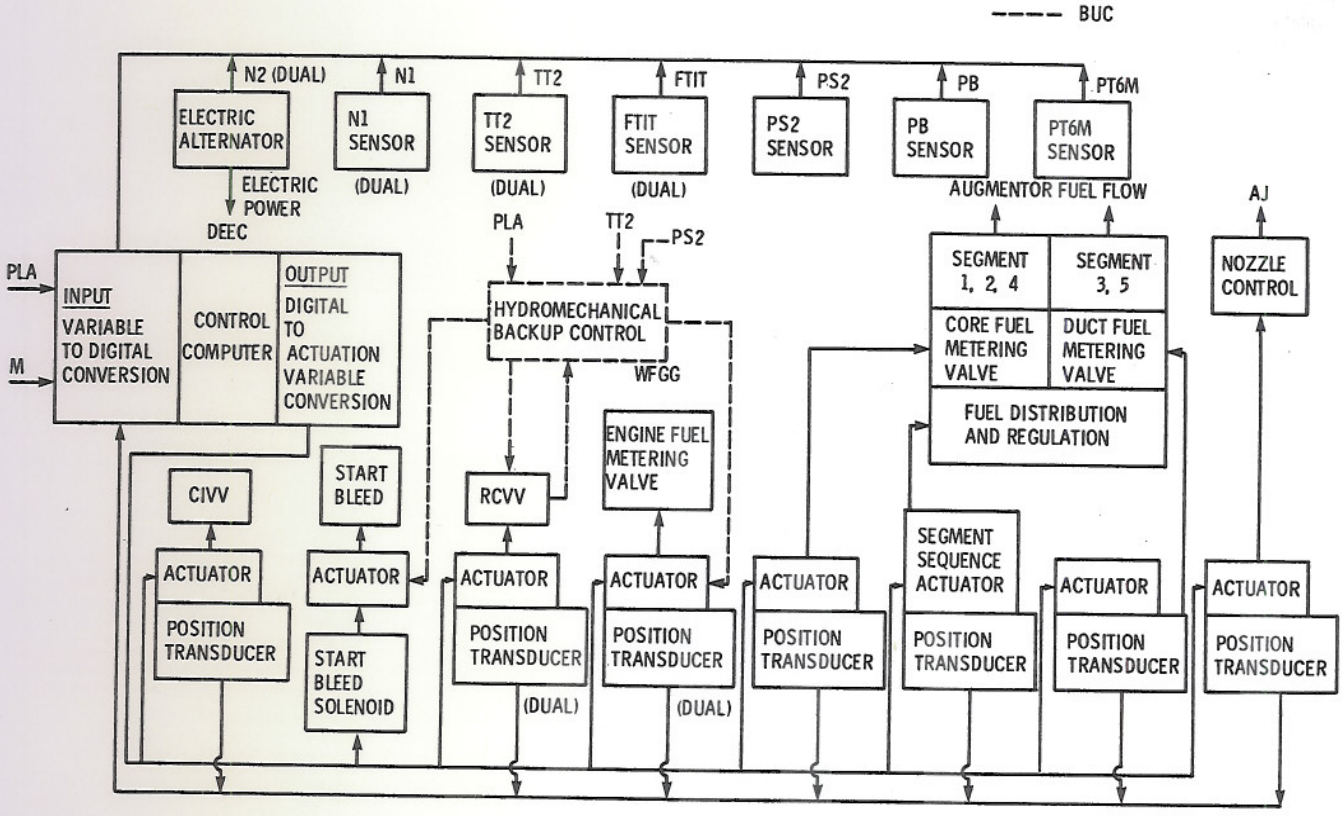

Figure 2. - Block diagram of the DEEC control system.

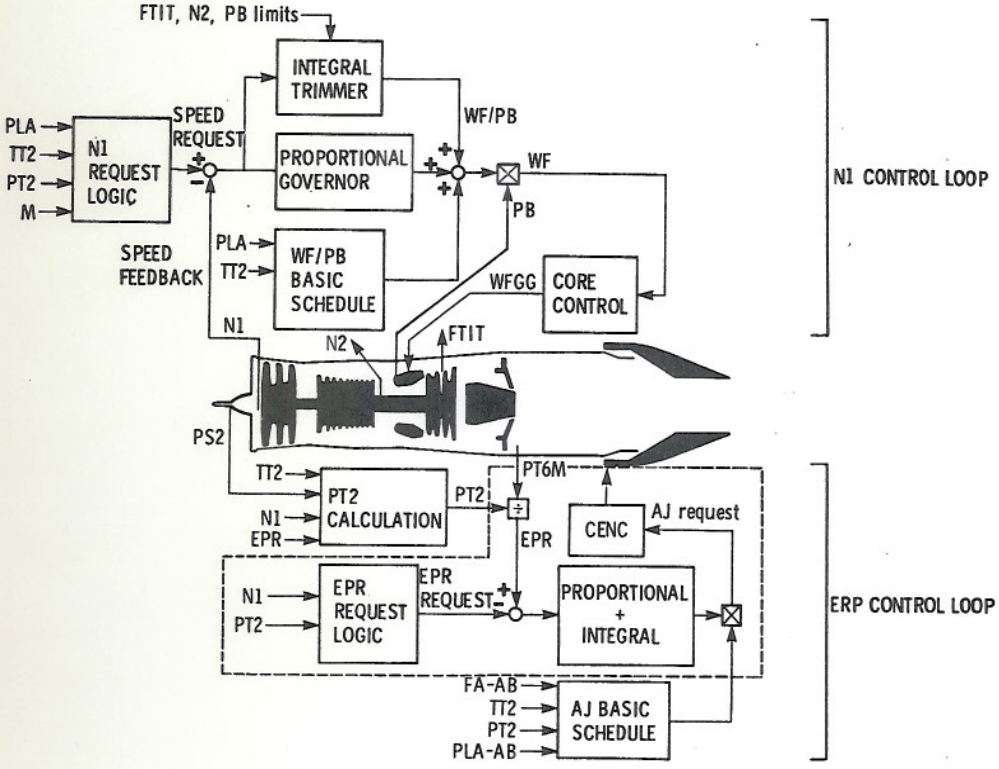

Figure 3. - DEEC basic closed loop control modes.

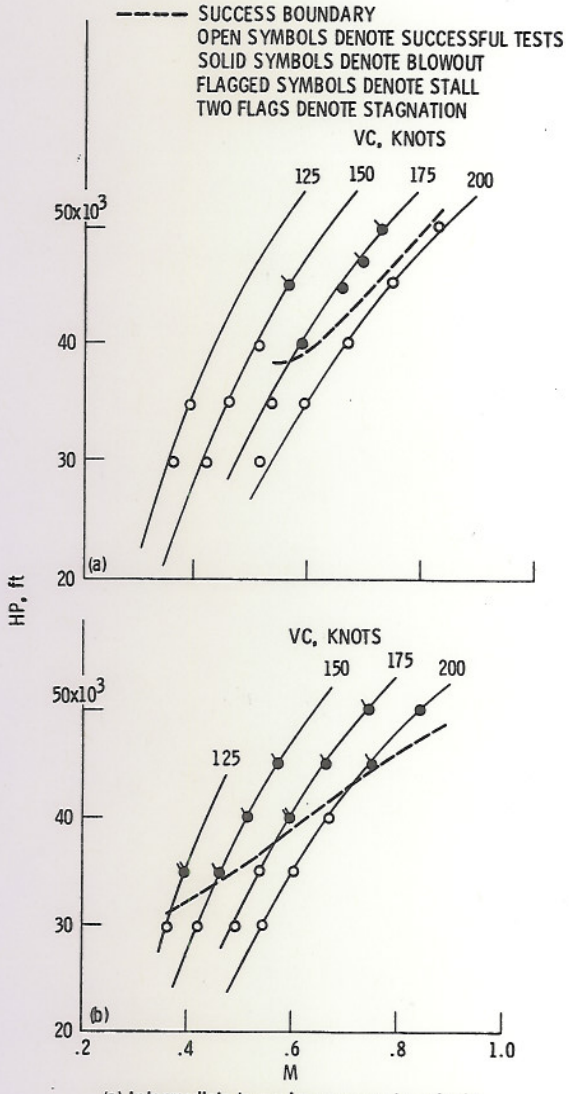

(a) Intermediate to maximum power transients.

(b) Idle to maximum power transients.

Figure 4. - Summary of DEEC augmentor transients, phase 2.

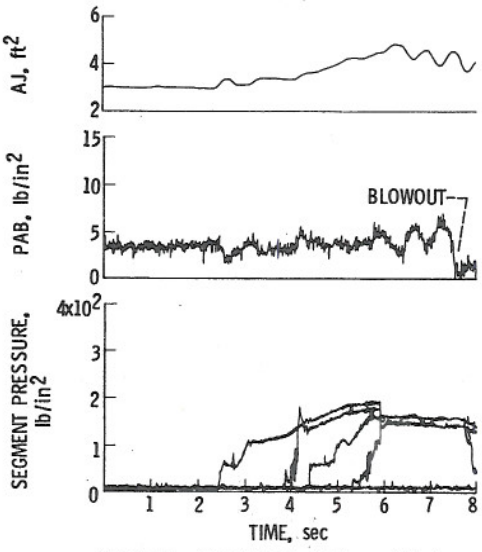

Figure 5. - Time history of intermediate to maximum power throttle transient in which nozzle instability caused an augmentor blowout. VC = 200 knots, HP = 50000 ft.

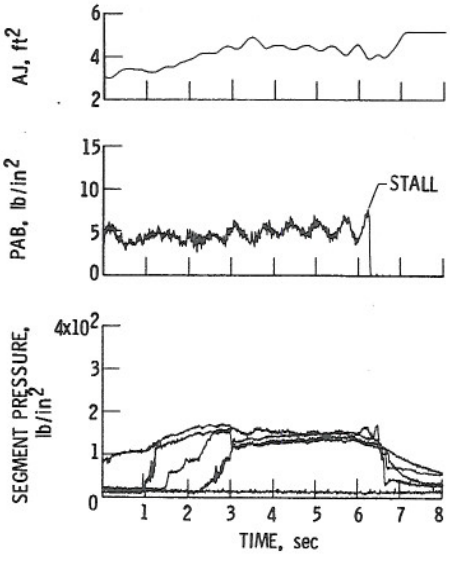

Figure 6. - Time history of an idle to maximum power throttle transient in which nozzle instability caused a stall. VC = 175 knots, HP = 45000 ft.

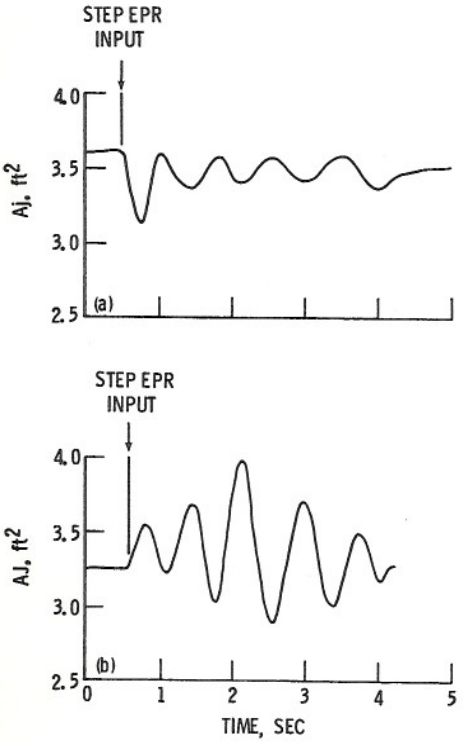

(a) Integral gain 2.5 times nominal.

(b) Integral gain 3.5 times nominal.

Figure 7. - Time history of nozzle response to step inputs in EPR, NASA Lewis tests of engine XD-11, HP = 45000 ft, M = 0.6.

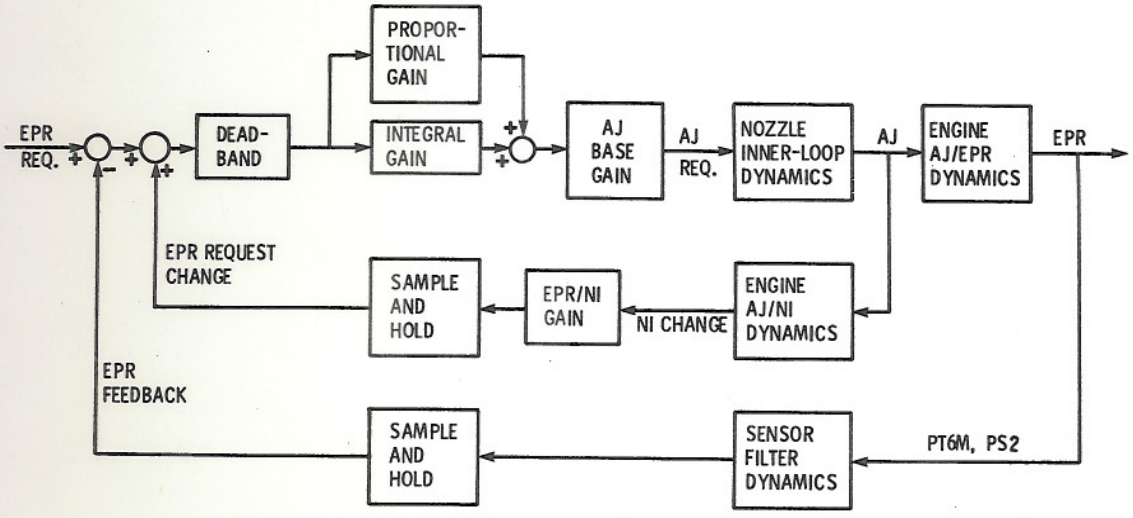

Figure 8. - Block diagram of the DEEC nonlinear digital nozzle simulation.

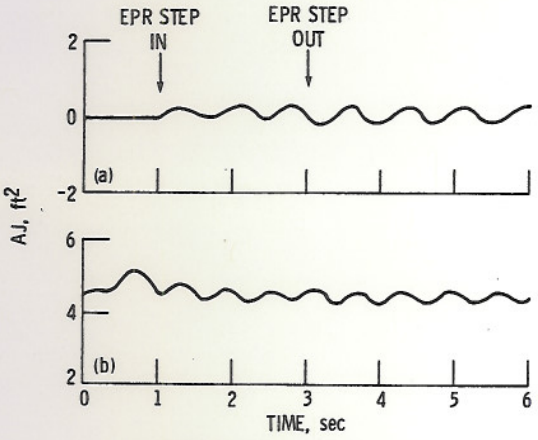

(a) Dryden nonlinear digital simulation.

(b) F-15 flight data from DEEC phase 2 tests.

Figure 9. - Time history of nozzle instability at M = 0.6, HP = 45 000 ft.

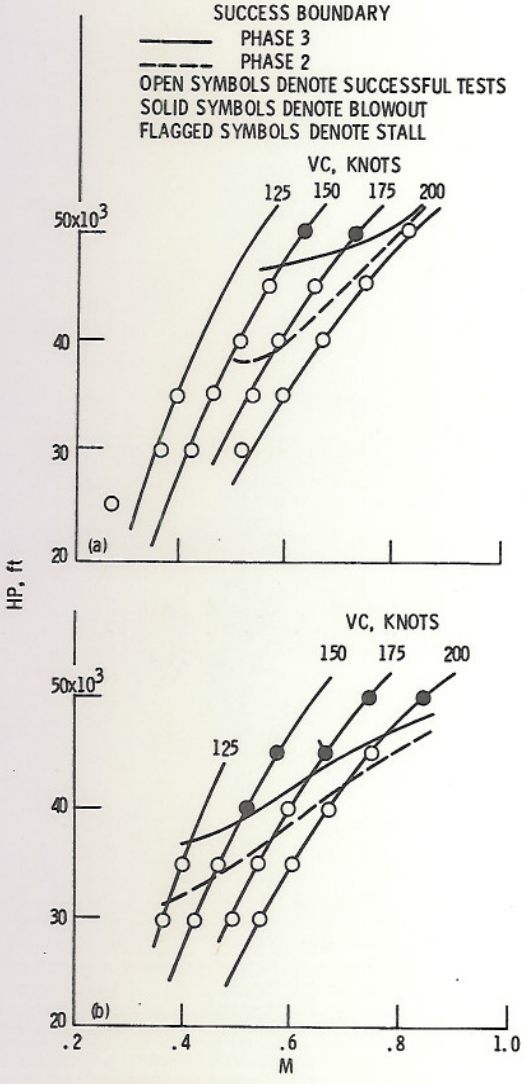

(a) Intermediate to maximum power transients.

(b) Idle to maximum power throttle transients.

Figure 10. - Comparison of augmentor transients from DEEC phases 2 and 3.

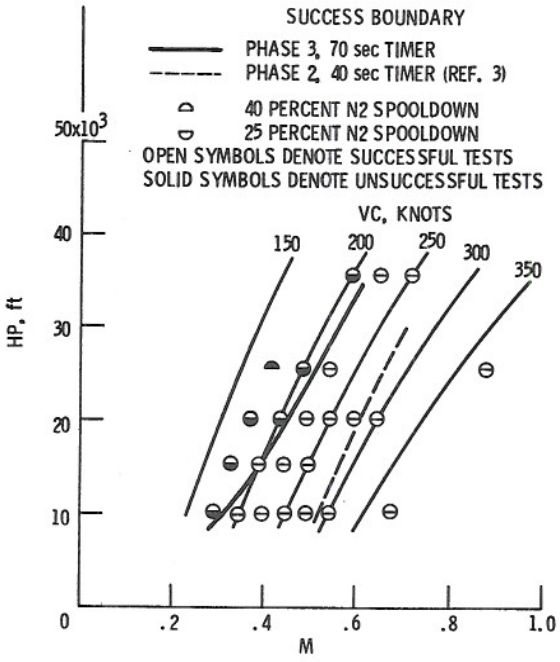

Figure 11. - Comparison of backup control airstart success for phase 2 and phase 3.

1. Report No. NASA TM-83088 AIAA-83-0537	2. Government Accession No.	3. Recipient's Catalog No.
4. Title and Subtitle FLIGHT EVALUATION OF MODIFICATIONS TO A DIGITAL ELECTRONIC ENGINE CONTROL SYSTEM IN AN F-15 AIRPLANE		5. Report Date 6. Performing Organization Code 505-34-02
7. Author(s) Frank W. Burcham, Jr. and Lawrence P. Myers		8. Performing Organization Report No. E-1515
9. Performing Organization Name and Address National Aeronautics and Space Administration Hugh L. Dryden Flight Research Facility, Edwards, California and Lewis Research Center, Cleveland, Ohio 44135		10. Work Unit No. 11. Contract or Grant No.
12. Sponsoring Agency Name and Address National Aeronautics and Space Administration Washington, D. C. 20546		13. Type of Report and Period Covered Technical Memorandum 14. Sponsoring Agency Code

15. Supplementary Notes

Frank W. Burcham, Jr. and Lawrence P. Myers, Hugh L. Dryden Flight Research Facility, Edwards, California and John R. Zeller, Lewis Research Center, Cleveland, Ohio. Prepared for the Twenty-First Aerospace Sciences Conference sponsored by the American Institute of Aeronautics and Astronautics, Reno, Nevada, January 10-13, 1983.

16. Abstract

The third phase of a flight evaluation of a digital electronic engine control system in an F-15 has recently been completed. It was found that DEEC software logic changes and augmentor hardware improvements resulted in significant improvements in engine operation. For intermediate to maximum power throttle transients, an increase in altitude capability of up to 8000 ft was found, and for idle to maximum transients, an increase of up to 4000 ft was found. A nozzle instability noted in earlier flight testing was investigated on a test engine at NASA Lewis Research Center. A DEEC software logic change was developed and evaluated, and no instability occurred in the Phase 3 flight evaluation. The backup control airstart modification was evaluated, and gave an improvement of airstart capability by reducing the minimum airspeed for successful airstarts by 50 to 75 knots.

17. Key Words (Suggested by Author(s)) Control Propulsion Digital	18. Distribution Statement Unclassified - unlimited STAR Category 07		
19. Security Classif. (of this report) Unclassified	20. Security Classif. (of this page) Unclassified	21. No. of Pages	22. Price*

* For sale by the National Technical Information Service, Springfield, Virginia 22161